Accepted for publication in Journal of Sound and Vibration, 1 May 2020.
Paper DOI: 10.1016/j.jsv.2020.115432

Differences between Euler-Bernoulli and Timoshenko beam formulations for calculating the effects of moving loads on a periodically supported beam

Xianying Zhang*[1], David Thompson[1] and Xiaozhen Sheng[2]

1 Institute of Sound and Vibration Research, University of Southampton, Southampton SO17 1BJ, UK

2 Shanghai University of Engineering Science, 333 Long Teng Road, Shanghai 201620, China

* Corresponding author: xianyingzhang96@gmail.com

Abstract

It is generally considered that a Timoshenko beam is superior to an Euler-Bernoulli beam for determining the dynamic response of beams at higher frequencies but that they are equivalent at low frequencies. Here, the case is considered of the parametric excitation caused by spatial variations in stiffness on a periodically supported beam such as a railway track excited by a moving load. It is shown that large differences exist between the results obtained using Timoshenko and Euler-Bernoulli beams for a railway track with typical parameters; the Euler-Bernoulli beam model underestimates this parametric excitation by around a factor of 3. This difference is shown to be due to shear deformation in the rail, which is significant for span lengths less than about 2 m. A 2.5D finite element model of the rail is used as a reference. This gives a deflection that is closer to the Timoshenko beam model. However, the displacement profile obtained from the Timoshenko beam model has a discontinuity of gradient at the support points, whereas neither the Euler-Bernoulli beam nor the 2.5D finite element model contains the discontinuity of gradient. Finally, the moving load is introduced explicitly in the various periodically supported models. The results for a moving constant load, expressed as an equivalent roughness, are not strongly affected by the load speed until the sleeper passing frequency approaches the vertical track resonance at which the track mass bounces on the support stiffness. Consequently, a quasi-static model gives satisfactory results for moderate load speeds.

Keywords: railway track; parametric excitation, Euler-Bernoulli beam, Timoshenko beam, periodically supported beam, moving load, 2.5D finite element method

1. Introduction

The Timoshenko beam formulation is generally considered to be more accurate than the Euler-Bernoulli beam for higher frequency problems. The inclusion of shear deformation and rotational inertia in the Timoshenko beam formulation leads to differences in their frequency responses, wavenumbers and hence natural frequencies, which become significant once the structural wavelength becomes comparable with the size of the cross-section [1]; for a rectangular cross-section this is typically smaller than 6 times the section height.

At low frequencies, however, the wavenumbers and mobilities obtained from the two beam formulations are very similar. It is therefore perhaps surprising to discover that there are substantial differences between the results of the two models in the response of a periodically supported railway track to a moving load, the so-called parametric excitation at the 'sleeper passing frequency'. The aim of this paper is to highlight and explore these differences.

Many models of railway track vibration represent the rails as beams [2,3]. Classical Euler-Bernoulli beam theory is widely used for low frequency dynamic problems, for example, to calculate the track deflections under moving loads [4], or in studies of ground vibration from trains [5,6], for which the frequency range of interest is below 250 Hz. For higher frequencies, however, the Timoshenko beam formulation is considered more reliable; for the vertical vibration of a rail, the Timoshenko beam formulation is preferred above approximately 500 Hz [2,3,7].

Although the rail supports are approximately periodically spaced, nevertheless a good approximation to the frequency response at most frequencies can be obtained by an equivalent continuous model [3]. The main exception to this is close to the pinned-pinned frequency, typically occurring at around 1 kHz for the vertical direction, at which half the bending wavelength equals the inter-sleeper distance. Grassie et al. [7] and Vincent and Thompson [8] compared measured receptances of a track with analytical frequency-domain models based on a beam, either continuously or discretely supported on rail pads, sleepers and ballast, and found good agreement when a Timoshenko beam is used. De Man [9] presented a finite element model of track in the frequency domain based on Timoshenko beam elements and also showed good agreement with measurements, including at the pinned-pinned resonance.

Another effect of the discrete support of the railway track is that the track stiffness varies within a sleeper bay. This can lead to a parametric excitation at the sleeper-passing frequency. An early study was carried out by Inglis [10] who approximated this parametric excitation by the variation in the quasi-static response of the system to a very slowly moving load. He also considered dynamic effects and showed that softer supports lead to a reduced range of movement.

Belotserkovskiy [11] presented an analytical model of a moving constant or harmonic load on an Euler-Bernoulli beam with periodic elastic supports. Nordborg [12] studied the parametric excitation by using an analytical frequency-domain formulation that included the moving load. The track was modelled using an Euler-Bernoulli beam with a reduced bending stiffness to ensure that the pinned-pinned frequency agreed with measurements [13]. Sheng et al. [14] introduced a wavenumber-based approach for the computation of the response of periodically supported structures to a moving harmonic load in the frequency domain and applied it to the vibration of a rail. For the vertical vibration, the rail was represented by a Timoshenko beam and for the lateral vibration it was represented by a multiple beam model. In an alternative approach, Wu and Thompson [15] studied parametric excitation of a railway track using a Timoshenko beam model, which was approximated by a rational polynomial function with variable coefficients to allow solution in the time domain.

Mazilu [16, 17] introduced an analytical method for the response of a periodic track based on Green's functions transformed from the frequency domain to the time domain. The results included the response to a moving mass representing the wheel, connected to the track through a contact spring. It was shown that the response has a maximum when the sleeper passing frequency is equal to the natural frequency of the coupled wheel/rail system. Sub-harmonic parametric resonance was also seen when the wheel velocity was one-half or one-third of the value corresponding to the main parametric resonance.

The problem of a moving load on a railway track can also be solved using numerical methods such as the finite element method in the time domain. Authors have variously used either Euler-Bernoulli beams [18-25] or Timoshenko beams [26-30] for this. In [29, 30], for example, FE models were used for a switch in which the rails were modelled using Timoshenko beams. As well as the impact loading at the crossing, Andersson and Dahlberg [29] observed variations in wheel load through each sleeper bay which can be associated with the parametric excitation. In a finite element model, however, the use of Timoshenko beams leads to a fictitious response

due to slope discontinuity at loading points, not present for Euler-Bernoulli beams. This was noted by Nielsen & Igeland [26] but they were able to neglect it as it is much smaller than the response to the roughness excitation or wheel flats that they studied. More recently, Koro et al. [31] and Yang [32] have introduced modified FE formulations of Timoshenko beams to overcome this fictitious response.

There have been many comparisons of Euler-Bernoulli beams and Timoshenko beams for various applications. For example, Lubaschagne et al. [33] compared models for a cantilever beam based on Euler-Bernoulli and Timoshenko beam theories and on two-dimensional elasticity. By comparing the natural frequencies and mode shapes, they concluded that the Timoshenko theory is close to the two-dimensional theory for modes of practical importance. Beck and da Silva [34] presented a comparison of the Euler-Bernoulli and Timoshenko beam theories for the example of a finite clamped-clamped beam, taking into account parameter uncertainties and uncertainty propagation and showed that the propagation of uncertainties was quite different in the two models.

Yavari et al. [35] studied moving loads on bridges modelled as beams. A discrete element technique was introduced and results were compared with those from finite element and finite difference methods. The Euler-Bernoulli and Timoshenko beam formulations were also compared and differences between them were only found to be significant when the beam slenderness is small, that is the square of length divided by the radius of gyration of the cross-section.

In the context of railway track, Grassie et al. [7] compared the frequency response of a railway track calculated using infinite Euler-Bernoulli and Timoshenko beam formulations and showed that the Timoshenko beam model was to be preferred above 500 Hz. Mosavi et al. [36] compared the Euler-Bernoulli and Timoshenko beam equations representing a track as an infinite beam on a Winkler foundation but did not give any results. Ruge and Birk [37] compared the Timoshenko and Euler–Bernoulli beam models of a rail on a continuous (Winkler) support under transient loading and concluded that the physically more realistic Timoshenko beam model also offers additional numerical advantages when dealing with transient dynamic problems in unbounded domains. Abe et al. [38] studied an instability occurring on a periodically supported track due to parametric excitation, particularly for light damping. They included a comparison of Euler-Bernoulli and Timoshenko beams for this problem and showed some differences in the critical speed. However, the magnitude of the stiffness variation (which

will be shown here to be a major difference between the two beam formulations) was taken as an input parameter which was assumed to be the same in both cases.

Despite the fact that many authors use either the Euler-Bernoulli beam or Timoshenko beam to study moving loads on a periodic railway track, the two approaches have not previously been compared in a systematic way for this problem. It is likely that, because the parametric excitation at the sleeper-passing frequency is a low frequency phenomenon, the two approaches are believed to be approximately equivalent. The aim of this paper is to investigate the differences in the parametric excitation occurring for a load moving along a periodic track using models based on Euler-Bernoulli beams and Timoshenko beams. The reasons for the discrepancies found are addressed by comparing the results with those obtained using a model of a discretely supported rail based on a 2.5D finite element (FE) model [39] which is used as a reference. The influence of the moving load speed on the parametric excitation is also explored. For simplicity, the study is limited to a moving constant load. Although the interaction with the unsprung mass of the wheel affects the magnitude of the excitation [16, 17], by expressing the parametric excitation as an equivalent roughness, the frequency-dependent excitation can also be taken into account. Consequently, the relative differences between the Euler-Bernoulli beam and Timoshenko beam will remain approximately the same because the track mobilities from the two models are very similar in this low frequency range.

First, in Section 2 the beam and 2.5D FE models are introduced and the point mobilities and wavenumbers of a discretely supported track are compared for the three models. Then, in Section 3, results at the sleeper-passing frequency are estimated using a quasi-static approach based on the variation of track deflections within a sleeper span. To minimise the effect of the vehicle-track interaction, the results are then expressed in the form of an equivalent roughness excitation. The effect of varying the support stiffness or the support spacing is also considered. Finally, in Section 4 the effect of the load speed is introduced explicitly using the Fourier series method of [14] for a moving constant load using the Euler-Bernoulli and Timoshenko beams as well as the 2.5D FE model.

2. Track models and point mobility

2.1 Free beam models

Consider first a free rail in vertical bending represented by either Euler-Bernoulli or Timoshenko beam models [1]. The equation of motion of an Euler-Bernoulli beam in the absence of damping excited by a point force is

$$EI\frac{\partial^4 u}{\partial x^4}+\rho A\frac{\partial^2 u}{\partial t^2}=F\mathrm{e}^{\mathrm{i}\omega t}\delta\left(x\right) \tag{1}$$

where E is Young's modulus, I is the second moment of area of the cross-section, ρ is the density of the beam and A the cross-sectional area. F is the amplitude of the external excitation force applied at x=0, while ω is the excitation frequency. u denotes the vibration amplitude of the beam, x is the distance along the beam and t is time.

The equations of motion for a Timoshenko beam can be written as

$$GA\kappa\frac{\partial}{\partial x}\left(\phi-\frac{\partial u}{\partial x}\right)+\rho A\frac{\partial^2 u}{\partial t^2}=F\mathrm{e}^{\mathrm{i}\omega t}\delta\left(x\right) \tag{2}$$

$$GA\kappa\left(\phi-\frac{\partial u}{\partial x}\right)-EI\frac{\partial^2\phi}{\partial x^2}+\rho I\frac{\partial^2\phi}{\partial t^2}=0 \tag{3}$$

where G is the shear modulus and κ is the shear coefficient. u is the deflection, while ϕ is the rotation of the cross-section relative to the undeformed axis.

The parameters for a UIC60 rail are listed in Table 1 together with the support properties that will be used later. For these parameters, below 500 Hz the difference in mobility is found to be less than 2.5% and the difference between the free wavenumbers is less than 7%.

2.2 Periodically supported beam models

Consider now a track consisting of a periodically supported beam. For simplicity, a single layer support is used in which each support is assumed to consist of a single damped spring for the rail pads; the sleepers, ballast or track slab are neglected. The track model is shown in Figure 1 and the parameters adopted are listed in Table 1.

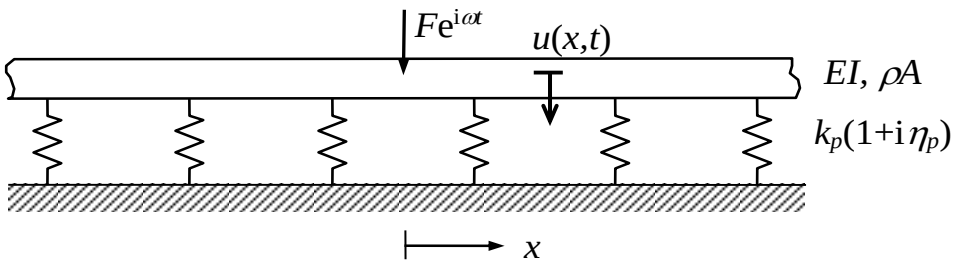

Figure 1 Model of discretely supported track.

Table 1 Parameters adopted for the track.

		Vertical
Rail bending stiffness	EI	6.42 MNm^2
Rail mass per unit length	ρA	60 kg/m
Rail shear stiffness*	GA	6.17×10^8 N
Rail shear parameter*	κ	0.4
Rail rotational inertia*	ρI	0.240 kgm
Rail damping loss factor	η	0.02
Pad stiffness	k_p	100 MN/m
Pad damping loss factor	η_p	0.2
Support spacing	d	0.6 m

*: not used for Euler-Bernoulli beam model.

The model for the discretely supported Timoshenko beam is described in [3,40]. The infinite beam is supported by a finite number of discrete springs; in this case 60 springs are used on each side of the force point. If $u(x)$ is the displacement of the beam at the point x and the beam is attached to supports of stiffness k_p at $x_n=nd$ for integer values of n, a reaction force, equal to $-k_p u(x_n)$, acts at each of these points. Here k_p is understood as the complex stiffness, i.e. implicitly including the term $(1 + \mathrm{i}\,\mathrm{sgn}(\omega)\eta_p)$, where the term $\mathrm{sgn}(\omega)$ is introduced to ensure causality [5]. The total response of the beam at x to a harmonic point force $F\mathrm{e}^{\mathrm{i}\omega t}$ applied at x_c is given by

$$u(x) = F\alpha(x, x_c) - k_p \sum_{-N}^{N} \alpha(x, x_n) u(x_n) \tag{4}$$

where $\alpha(x, x_c)$ is the transfer receptance of the unsupported beam between a force at x_c and the displacement at x. The displacement $u(x_m)$ at the support point x_m can be written as

$$u(x_m) = F\alpha(x_m, x_c) - k_p \sum_{-N}^{N} \alpha(x_m, x_n) u(x_n) \tag{5}$$

This can be rearranged into a matrix equation

$$\left(\mathbf{I}+k_p\boldsymbol{\alpha}\left(x_m,x_n\right)\right)\cdot\mathbf{u}\left(x_n\right)=F\boldsymbol{\alpha}\left(x_m,x_c\right) \tag{6}$$

where $\boldsymbol{\alpha}(x_m, x_n)$ is a square matrix consisting of point and transfer receptances of the free beam, $\mathbf{I}$ is a unit matrix, $\mathbf{u}(x_n)$ is a vector of the displacements at the support points x_n and $\boldsymbol{\alpha}(x_m, x_c)$ is a vector of the transfer receptances between the excitation point x_c and the support points x_m. This can be solved for $\mathbf{u}(x_n)$ by applying a matrix inversion and then the response at a general position x can be obtained by substituting back into Equation (4). The point and transfer receptances of the infinite beam can be calculated for either the Euler-Bernoulli beam or the Timoshenko beam using this method.

2.3 2.5D finite element model

A 2.5D finite element model (also known as waveguide FE or semi-analytical FE model) [41] of the rail is used for comparison. This approach is briefly described here; further details can be found in [41]. Consider a structure which is invariant in one direction, here denoted the x-direction, and has an arbitrary cross-section in the (y, z) plane, which is discretised into finite elements. The partial differential equation of the structure can be written as

$$\left[\mathbf{K_2}\frac{\partial^2}{\partial x^2}+\mathbf{K_1}\frac{\partial}{\partial x}+\mathbf{K_0}+\mathbf{M}\frac{\partial^2}{\partial t^2}\right]\mathbf{U}(x,t)=\mathbf{F}(x,t) \tag{7}$$

where $\mathbf{K_2}$, $\mathbf{K_1}$ and $\mathbf{K_0}$ are stiffness matrices and $\mathbf{M}$ is the mass matrix of the cross-section; $\mathbf{U}(x, t)$ is the vector of displacements of FE node points on the cross-section and $\mathbf{F}$ is the corresponding external force vector. Since the structure is invariant in the x direction, all the matrices in the equation are independent of x. Assuming harmonic motion with respect to time at frequency ω and with respect to the x coordinate with wavenumber k_x, the displacement vector can be written as $\mathbf{U}(x,t)=\tilde{\mathbf{U}}e^{i(\omega t-k_x x)}$ and Equation (7) becomes

$$[\mathbf{K_2}(-\mathrm{i}k_x)^2+\mathbf{K_1}(-\mathrm{i}k_x)+\mathbf{K_0}-\omega^2\mathbf{M}]\tilde{\mathbf{U}}=\tilde{\mathbf{F}} \tag{8}$$

where $\tilde{\mathbf{U}}$ and $\tilde{\mathbf{F}}$ are the displacement amplitudes of the nodes and the corresponding amplitudes of the external forces in the wavenumber domain, respectively. Equation (8) can be solved to obtain the response $\tilde{\mathbf{U}}$ at each wavenumber and frequency. The spatial distribution of the displacement $\mathbf{U}(x)$ can then be recovered by a Fourier transform:

$$\mathbf{U}(x)=\frac{1}{2\pi}\int_{-\infty}^{\infty}\tilde{\mathbf{U}}\,(k_x)e^{-\mathrm{i}k_x x}\mathrm{d}k_x \tag{9}$$

The free rail is represented using this method by 11 eight-node elements, as shown in Figure 2.

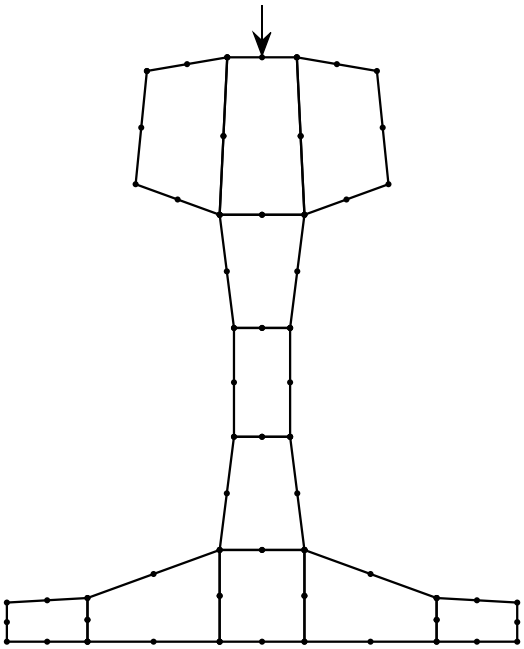

Figure 2 Finite element mesh used for rail cross-section.

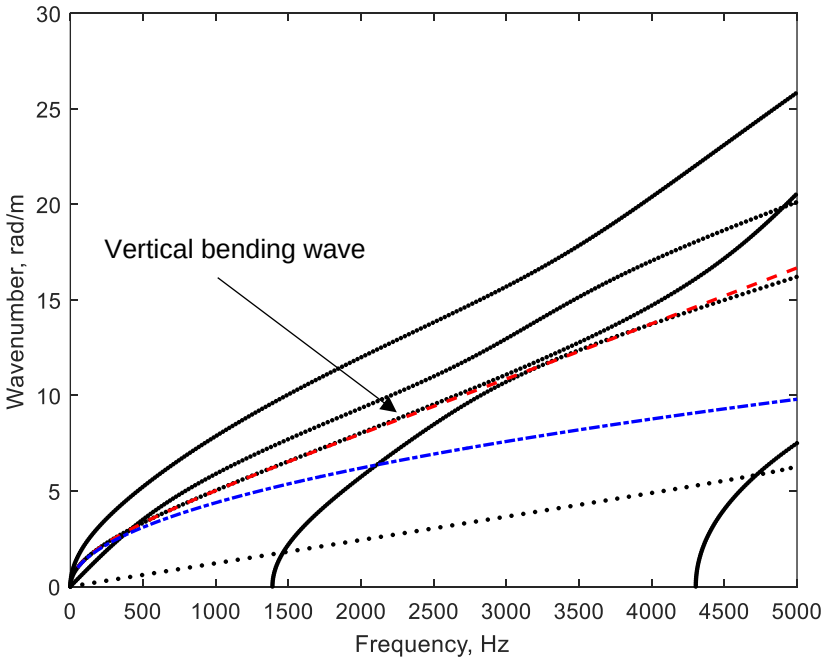

Figure 3 Dispersion curves of unsupported beams. …, from 2.5D FEM; ———, from Timoshenko beam model; –·–, from Euler-Bernoulli beam model

2.4 Results

The wavenumbers of the free waves in this rail are shown in Figure 3 as discrete points at a spacing of 0.1 rad/m. These are obtained from Equation (8) by setting $\tilde{\mathbf{F}} = \mathbf{0}$ and solving for ω at each value of k_x. They are compared with the wavenumbers obtained from the beam models. The wavenumber from the Timoshenko beam model is similar to that of the vertical bending wave obtained from the 2.5D FE model up to about 3 kHz. The Timoshenko beam also has a second propagating wave but this cuts on above 5 kHz for the current parameters. The Euler-Bernoulli beam, however, differs from the other models above about 500 Hz, as noted above. Other waves obtained from the 2.5D FE model, from highest to lowest, are lateral bending, torsion, longitudinal waves and two higher order waves involving bending of the cross-section [3].

The mobility of the discretely supported rail is calculated using the method described in Section 2.2 in which a finite number of supports are added to the bottom of the rail and the full system is solved using a receptance coupling method [39]. For the FE model, at each support point three springs of approximately equal stiffness are included across the width of the rail foot. There are 60 supports on each side of the excitation point for each model. The mobility at mid-span is compared with the results from the beam models in Figure 4. It can be seen that the results from the Timoshenko beam model agree well with those from the 2.5D model, especially for frequencies up to 1 kHz. The results all show a resonance peak at 265 Hz caused by bouncing of the rail mass on the support stiffness. Below the resonance peak, the track mobility is stiffness-controlled and is slightly higher for the Timoshenko beam and 2.5D models, especially at mid-span. The peak found at 1425 Hz for the Euler-Bernoulli beam and 1070 Hz for the other models is the first pinned-pinned mode. These differences are caused by the differences in wavenumber observed in Figure 3. There are some differences in the mobility magnitude at high frequencies and the phase of the 2.5D model diverges from that of the Timoshenko beam model above 1.5 kHz where cross-section deformation starts to become important. Similar agreement is found between the responses above a sleeper (not shown).

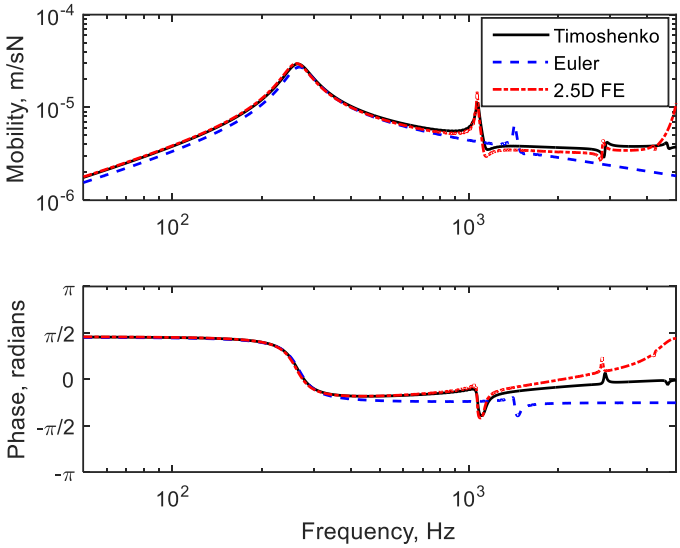

Figure 4 Comparison of point mobility at mid-span for Timoshenko and Euler beams and 2.5D FE model.

3. Simple estimate of parametric excitation

3.1 Estimate of variations within a span

When a wheel load runs over the rail, it can excite track and wheel vibration due to variations in the track stiffness within a sleeper span. As the rail receptance is approximately independent of frequency below 100 Hz, and determined by the inverse of the track stiffness, for low speeds this parametric excitation can be estimated from the variation in the quasi-static track deflection within a sleeper span. The same models as above can be used to find the quasi-static deflection from the receptance for frequencies tending to 0. These models do not include the effect of speed; this will be considered in Section 4 below. For simplicity, the comparison between the different models is limited to a moving constant load; although the interaction with the unsprung mass of the wheel affects the magnitude of the excitation [16, 17], these dynamic effects can be expected to be similar for the various models as their track mobilities are very similar below 500 Hz. Results are again shown for the single layer support, as shown in Figure 1, with the parameters given in Table 1.

Figure 5 shows the results of the three models in terms of the quasi-static track deflection at different positions in a span for a unit load. This is shown as positive downwards and for clarity three spans are shown. It can be seen that the variations in deflection are much greater for the Timoshenko beam than for the Euler-Bernoulli beam and the mean value is also greater. The variation in the results for the 2.5D model is similar in magnitude to that for the Timoshenko

beam. For the present parameters the deflection above the supports is 2.4% smaller than the mid-span results for the Euler-Bernoulli beam and this difference is 8.2% for the Timoshenko beam and 5.7% for the 2.5D FE model. Moreover, the variations for the Euler-Bernoulli beam are approximately sinusoidal whereas for the Timoshenko beam the slope is discontinuous at the support points [31, 32]. The results from the 2.5D model are similar to those of the Timoshenko beam model but do not exhibit the discontinuity in gradient at the support points, confirming that it is unphysical.

This discontinuity in slope is a consequence of the fact that the shear force in the Timoshenko beam depends on the first derivative of the beam displacement and on the rotation of the cross-section ($F=GA\kappa(\partial u/\partial x-\phi)$). In this way, because the rotation of the cross-section (ϕ) must be a continuous function, the presence of a concentrated force introduces a discontinuity in the slope of the beam ($\partial u/\partial x$). For the Euler-Bernoulli model the shear force depends on the third derivative of the beam displacement ($F=EI\partial^3 u/\partial x^3$) and a concentrated force introduces a discontinuity in that derivative; the first and second derivatives of the beam displacement remain continuous functions.

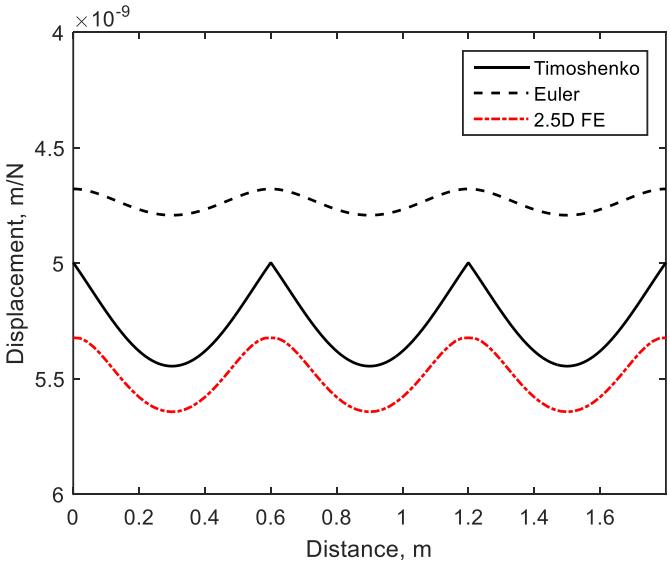

Figure 5 Variation of quasi-static deflection with position within three support spans

The periodic variations in deflection can be expanded into a Fourier series, the coefficients of which are shown in Figure 6 for the three models. The zero-order term, which corresponds to twice the average deflection over the span, is almost the same in each case. The first-order term, which corresponds to the amplitude of the variation at the sleeper-passing frequency, is 5.8×10^{-11} m/N for the Euler-Bernoulli beam and 2.0×10^{-10} m/N for the Timoshenko beam. Thus,

although the peak-to-trough amplitude is four times greater for the Timoshenko beam, the component at the sleeper-passing frequency is only three times greater due to the presence of the higher harmonics. For the 2.5D model this first-order term is 1.6×10^{-10} m/N, which is similar to the Timoshenko beam. The second-order term is more than an order of magnitude greater for the Timoshenko beam than for the Euler-Bernoulli beam and the higher order terms then reduce much less rapidly for the Timoshenko beam than for the Euler-Bernoulli beam as a consequence of the discontinuity in gradient seen in Figure 5. The results for the 2.5D model lie between those of the two beam models.

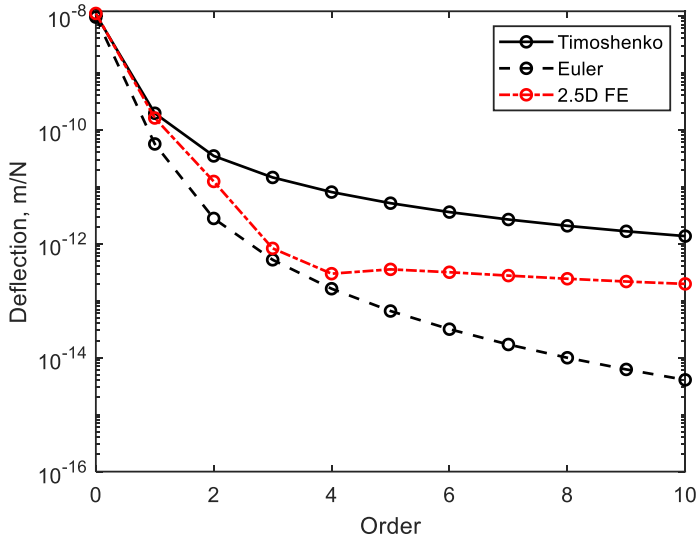

Figure 6 Fourier series of deflection variation within one span.

3.2 Estimate of equivalent roughness

The variations in stiffness within a sleeper span can be equated to an equivalent roughness excitation [3]. At low frequencies the wheel can be represented simply by a mass M_w and a static load F_0. For a perfectly smooth wheel and rail, where the support stiffness provided by the rail, $K(x)$, varies with distance x, the response of the wheel can be written as a quasi-static deflection of the track u_0 and a dynamic component u. This satisfies

$$M_w\ddot{u} + K(x)(u_0 + u) = F_0 \tag{10}$$

If the stiffness consists of a steady value K_T, and a small sinusoidal variation, $\delta K\sin(2\pi x/\lambda)$, this can be written as

$$M_w\ddot{u} + K_T\left(u_0 + u\right) + \delta K u_0 \sin\left(\frac{2\pi x}{\lambda}\right) = F_0 \tag{11}$$

where the products of the small quantities have been neglected.

As $K_T u_0 = F_0$, Equation (11) can be expressed as

$$M_w\ddot{u} + K_T u = -\left(\frac{\delta K}{K_T}\right) F_0 \sin\left(\frac{2\pi x}{\lambda}\right) \tag{12}$$

The steady-state response at frequency ω, corresponding to the wavelength λ has the amplitude

$$u = -\left(\frac{\delta K}{K_T}\right)\frac{F_0}{K_T - M_w\omega^2} \tag{13}$$

The simplest way of including the excitation due to the sleeper-passing frequency is to add it to the roughness spectrum at the sleeper-passing wavelength. In this way the dynamic interaction effects are also included. The displacement response amplitude of the rail and wheel to excitation by a harmonic roughness of amplitude r can be written as [3]

$$u_r = \frac{-\omega^2 M_w r}{(K_T - \omega^2 M_w)}, \; u_w = \frac{K_T r}{(K_T - \omega^2 M_w)} \tag{14}$$

where the rail and wheel receptances have been approximated by $1/K_T$ and $-1/\omega^2 M_w$ and the contact stiffness has been omitted. Equating these expressions to Equation (13) allows the equivalent roughness to be obtained. The resulting equivalent roughness for the rail and wheel responses are different. The equivalent roughness for the rail is

$$r_{req} = \left(\frac{\delta K}{K_T}\right)\frac{F_0}{M_w\omega^2} \tag{15}$$

and that for the wheel is

$$r_{weq} = -\left(\frac{\delta K}{K_T}\right)\frac{F_0}{K_T} \tag{16}$$

The two formulae give equivalent values at the wheel-track system resonance frequency (or P2 frequency) at which $K_T = \omega^2 M_w$ and which typically occurs at around 60 Hz.

For the track parameters considered above, the average track stiffness, K_T, is 211 MN/m for the Euler-Bernoulli beam, 190 MN/m for the Timoshenko beam and 182 MN/m for the 2.5D

model. The relative variation $\delta K/K_T$ within a sleeper span, derived from the Fourier coefficients, has an amplitude of ±1.2%, ±3.7% and ±2.9% respectively. For a static wheel load F_0 of 50 kN this leads to an equivalent roughness amplitude (for the wheel) from Equation (16) of ±2.9 μm for the Euler-Bernoulli beam, ±10.1 μm for the Timoshenko beam and ±8.0 μm for the 2.5D FE model.

Table 2 lists these values and the corresponding results for a range of support stiffness values for the three models. As the support stiffness increases, the relative amplitude of the stiffness variation increases approximately in proportion to the support stiffness [10]. However, due to the presence of K_T in the denominator of Equation (16), the equivalent roughness (for the wheel) only increases by a factor of around 2 for an order of magnitude increase in support stiffness. The equivalent roughness also increases in direct proportion to the wheel load. As can be seen from Table 2, the results from the Timoshenko beam model are slightly higher than those from the finite element model whereas the results from the Euler-Bernoulli beam model are around a factor of three lower.

Table 2 Effect of support stiffness (k_p) on average track stiffness (K_T), amplitude of relative variation in stiffness ($\delta K/K_T$) and amplitude of equivalent roughness (r_{weq}).

	Euler beam			Timoshenko beam			2.5D FE model		
k_p MN/m	K_T MN/m	$\delta K/K_T$	r_{weq} μm	K_T MN/m	$\delta K/K_T$	r_{weq} μm	K_T MN/m	$\delta K/K_T$	r_{weq} μm
25	75	0.26%	1.7	71	0.90%	6.4	70	0.73%	5.3
50	126	0.56%	2.2	117	1.84%	7.9	114	1.48%	6.5
100	211	1.19%	2.8	190	3.72%	9.8	182	2.93%	8.1
200	353	2.55%	3.6	303	7.40%	12.2	282	5.58%	9.9
400	589	5.40%	4.6	471	14.0%	14.9	416	9.90%	11.9

3.3 Effect of support spacing

The high frequency dynamic response of a Timoshenko beam diverges from that of an Euler-Bernoulli beam due to shear deformation when the wavelength becomes short. From Figure 3 and Figure 4, the two models diverge for a rail above about 500 Hz, which corresponds to a wavenumber of about 3 rad/m, i.e. a wavelength of about 2 m. In the discretely supported model, under a static load the rail bends between the supports. It is therefore hypothesised that the differences between the two models are associated with the ‘wavelength’ of this bending.

To test this, cases have been run using the two beam models with different values of support spacing. For convenience, the stiffness of each support has been adjusted to maintain the same stiffness per unit length. The average deflection of the rail over a span and the amplitude of the variation over the span (determined from the Fourier coefficients) are plotted in Figure 7. This shows that the amplitude of displacement variation increases with increasing span length (Figure 7(b)) and the average displacement increases for span lengths greater than 1.2 m (Figure 7(a)). Importantly, the results for the Timoshenko beam and Euler-Bernoulli beam converge for large values of the span length but there are large differences when the span length is small. Figure 7(c) shows the ratios between the results for the two models. For span lengths greater than 2 m the ratio between the amplitude obtained from the two models is greater than 0.9, i.e. the models agree to within less than 10%. This limit of 2 m agrees with the wavelength noted from (i.e. a wavenumber of 3 rad/m). Thus it can be seen that the difference between the two models is associated with shear deformation occurring for bending within short span lengths. Even though the frequency is low, the ‘wavelength’ of this deformation is no longer sufficiently large compared with the size of the cross-section to neglect shear deformation.

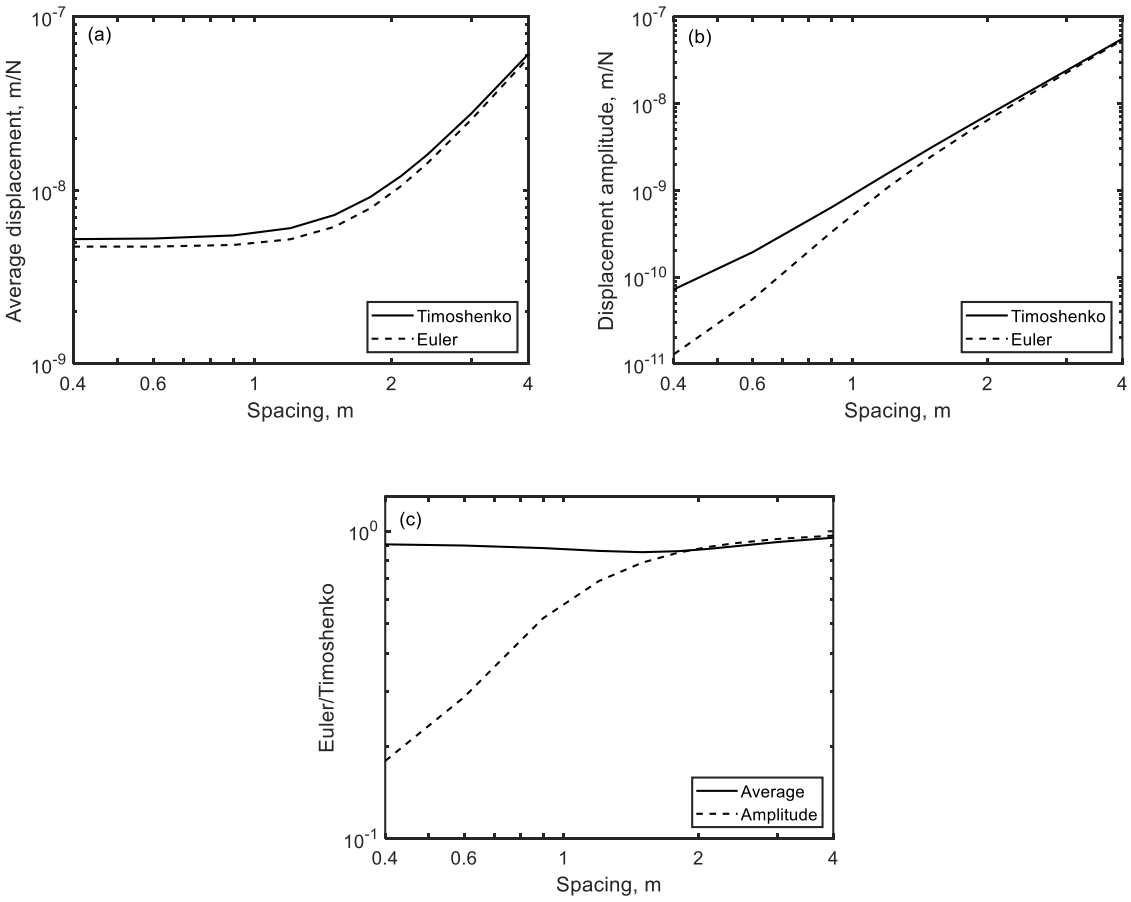

Figure 7 Effect of varying support spacing keeping a constant stiffness per unit length. (a) Average displacement per unit load; (b) displacement amplitude per unit load; (c) ratio of results for Euler-Bernoulli beam to those for Timoshenko beam.

4. Effect of moving load speed on the track deflections

In the results in the previous section the moving load is approximated by a static load applied at different positions within the span length [10]. In this section, to include the effect of load speed explicitly, the method of Sheng et al. [14] is used. This describes the response to a moving load of a 2.5D structure with a set of periodic supports. Although Ref. [14] also allows for a harmonic load, only the case of a constant moving load is considered here. The Euler-Bernoulli and Timoshenko beams are introduced into the same framework by describing them by 2.5D mass and stiffness matrices and the results are compared with those for the 2.5D FE model of the rail shown in Figure 2. The parameters are the same as used previously, as listed in Table 1. The calculations are based on integrals over wavenumber [14]; in the present calculations the maximum wavenumber is set to ±200 rad/m with 1024 steps. For the FE model,

only 10 supports on each side are used in the calculations in order to save computation time; there are again three springs at each support across the rail width. The maximum wavenumber is ±200 rad/m with 256 steps. It has been verified that this range is sufficient to achieve convergence.

In Figure 8 the track deflections at the loading point obtained by using the Timoshenko beam are shown for four different speeds, including the quasi-static result (actually calculated for a speed of 0.4 m/s to avoid numerical difficulties). This quasi-static result is almost identical to that calculated in Section 3, and shown in Figure 5, the remaining differences being due to the wavenumber resolution used here. At 40 m/s the track deflection is very similar to the quasi-static result but at higher speeds the results are modified by the track dynamic behaviour.

Figure 9 shows the Fourier coefficients of these deflections. The zero and first order terms are virtually unaffected by the load speed but higher order terms are influenced to some extent. At 40 m/s the sleeper-passing frequency corresponds to 66.7 Hz and the fourth order to 267 Hz, which coincides closely with the peak in the rail mobility seen in Figure 4. The track dynamic behaviour therefore leads to a slightly higher response in the fourth order and lower responses at orders 5 and above. At 80 m/s the slight peak occurs at the second order (corresponding to 267 Hz) and the amplitude is lower for orders 3 and above, while for 160 m/s the sleeper-passing frequency (i.e. order 1) corresponds to 267 Hz.

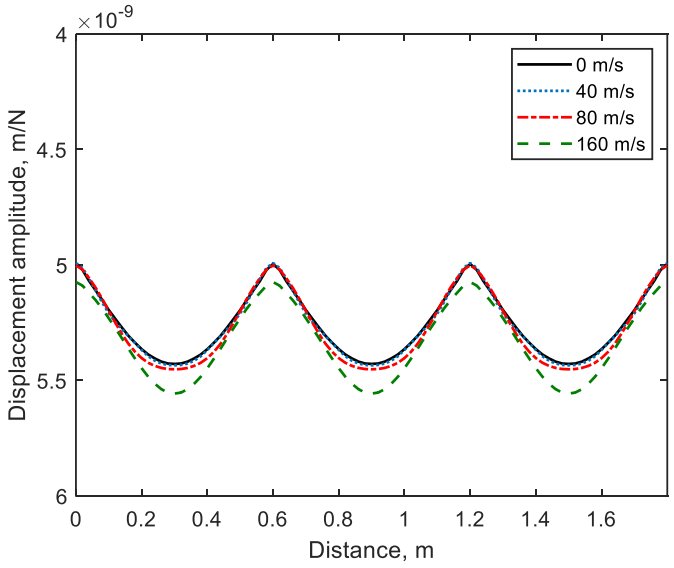

Figure 8 Variation of track deflection with position within a support span for a Timoshenko beam for a load moving at different speeds

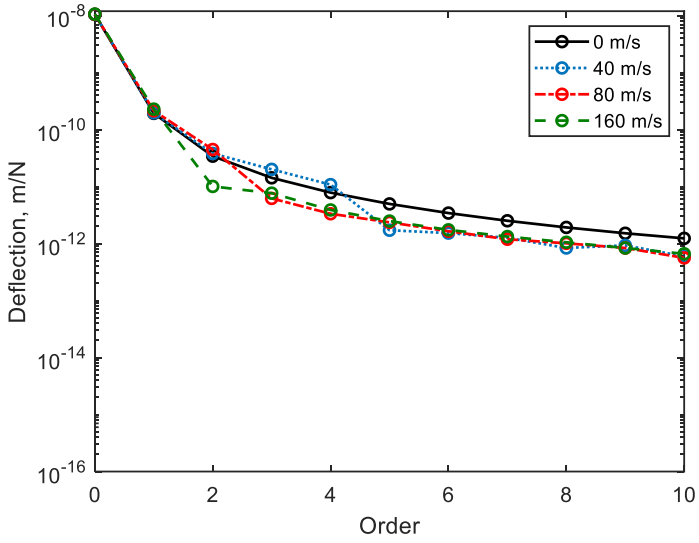

Figure 9 Fourier series of deflections within one span for a Timoshenko beam for a load moving at different speeds.

The track deflections for the Euler-Bernoulli beam model are shown in Figure 10 for these four speeds. The deflection is hardly affected by the speed, apart from an increase in the mean deflection at 160 m/s. The Fourier coefficients are shown in Figure 11. These show similar variations due to speed as those for the Timoshenko beam, i.e. slight peaks when the frequency equals that of the track resonance. As seen in Figure 6 the spectral levels drop more rapidly than for the Timoshenko beam. The corresponding results for the 2.5D FE rail model are presented in Figure 12 and Figure 13. Again, there is a small influence due to the dynamic behaviour for the higher speeds, similar to the results of the Timoshenko beam model. Table 3 summarises the results in terms of the same parameters as previously, from which it is clear that the results are hardly affected by the load speed except for the 160 m/s case where the sleeper-passing frequency coincides with the track resonance.

Generally, it can be concluded that, as long as the track dynamic response is in the stiffness-controlled region, i.e. below the first track resonance frequency, the sleeper-passing effect due to a moving load can be estimated adequately using a quasi-static approach. Thus, the results taking account of the moving load confirm those from the quasi-static calculations and show that the Euler-Bernoulli beam gives a parametric excitation around three times too small.

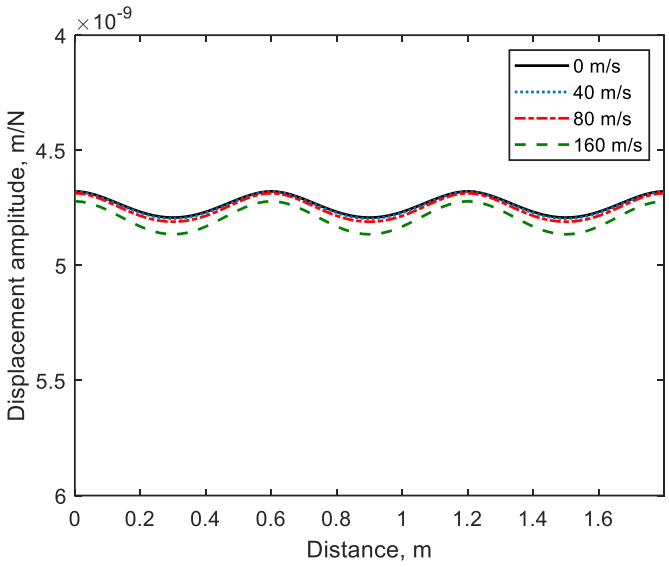

Figure 10 Variation of track deflection with position within a support span in an Euler-Bernoulli beam for a load moving at different speeds

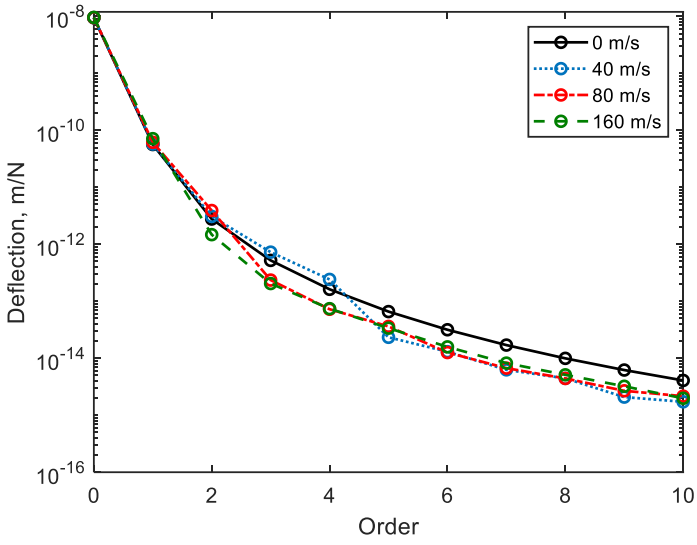

Figure 11 Fourier series of deflections within one span for an Euler-Bernoulli beam for a load moving at different speeds.

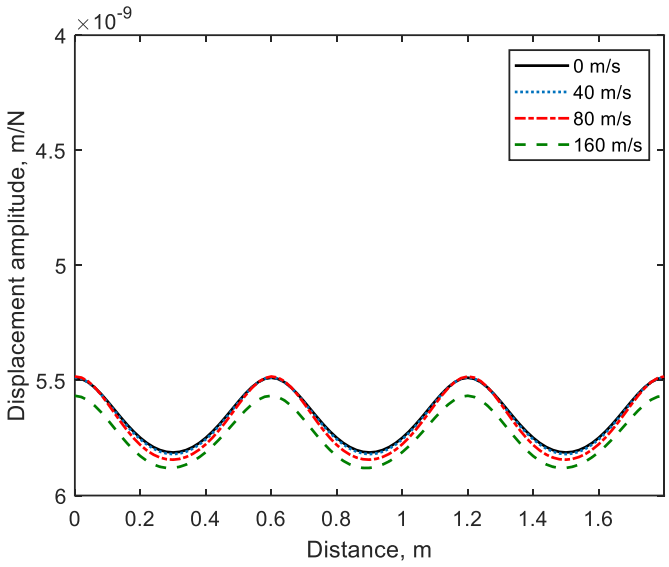

Figure 12 Variation of track deflection with position within a support span in a 2.5D FE rail for a load moving at different speeds

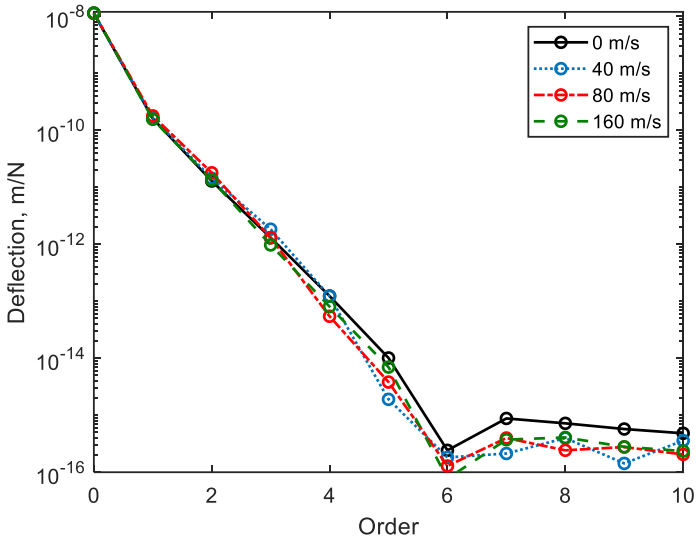

Figure 13 Fourier series of deflections within one span in a 2.5D FE rail for a load moving at different speeds.

Table 3 Effect of load speed on average track stiffness (K_T), amplitude of relative variation in stiffness ($\delta K/K_T$) and amplitude of equivalent roughness (r_{weq}) for k_p = 100 MN/m and F_0 = 50 kN.

	Euler-Bernoulli beam			Timoshenko beam			2.5D FE model		
Load speed, m/s	K_T MN/m	$\delta K/K_T$	r_{weq} μm	K_T MN/m	$\delta K/K_T$	r_{weq} μm	K_T MN/m	$\delta K/K_T$	r_{weq} μm
0	211.1	1.19%	2.82	190.2	3.70%	9.73	176.6	2.85%	8.07
40	210.9	1.21%	2.88	190.1	3.78%	9.94	176.5	2.92%	8.27
80	210.4	1.30%	3.09	189.6	4.09%	10.79	176.1	3.17%	9.00
160	208.6	1.49%	3.57	187.7	4.31%	11.48	174.4	2.73%	7.83

5. Conclusions

By comparing the parametric excitation occurring for a moving load on either an Euler-Bernoulli beam or a Timoshenko beam on a periodic support with a 2.5D FE model used as a reference, it is shown that, for typical parameters, the Euler-Bernoulli beam model underestimates this parametric excitation by around a factor of 3. This difference is shown to be due to shear deformation in the rail, which is found to be significant for span lengths less than about 2 m.

The displacement profile obtained from the Timoshenko beam model also exhibits an unphysical discontinuity in the gradient at the support points [31, 32]. This leads to greater high frequency components so, although the component at the sleeper passing frequency is quite well predicted, the higher frequency components are significantly overestimated. This discontinuity can be reduced by introducing multiple springs to represent each support point, as proposed by [42-44].

By introducing the moving load explicitly in the various periodically supported models it is shown that the results for a moving constant load are not strongly affected by the load speed until the sleeper passing frequency approaches the vertical track resonance frequency at which the rail mass bounces on the support stiffness. The quasi-static approach to modelling the sleeper-passing effect for a moving load gives satisfactory results for speeds up to 40 m/s in the example shown, and even at higher speeds the error is not large. For the response due to moving harmonic loads or the interaction with moving wheels, however, a more complete model, e.g. [14, 45], should be used.

The results of this study show clearly that to consider the parametric excitation of a railway track due to the sleeper passing effect, at least a Timoshenko beam including shear deformation should be used. An Euler-Bernoulli beam formulation leads to considerable underestimates of the effect, which does not appear to have been previously recognised.

All data published in this paper are openly available from the University of Southampton repository at https://doi.org/10.5258/SOTON/D1362

Acknowledgements

The work described here has been supported by the Ministry of Science and Technology of China under the National Key R&D Programme grant 2016YFE0205200, 'Joint research into key technologies for controlling noise and vibration of high-speed railways under extremely complicated conditions', and the Engineering and Physical Sciences Research Council of the UK (EPSRC) under the programme grant EP/M025276/1, 'The science and analytical tools to design long life, low noise railway track systems (Track to the Future)'.

References

[1] K.F. Graff, Wave motion in elastic solids, Dover Publications, New York, 1991.

[2] K. Knothe, S.L. Grassie, Modelling of railway track and vehicle/track interaction at high frequencies, Vehicle System Dynamics. 22 (1993) 209-262.

[3] D. Thompson, Railway noise and vibration: mechanisms, modelling and means of control, Elsevier: Oxford, 2008.

[4] D.R.M. Milne, L.M. Le Pen, D.J. Thompson, W. Powrie, Properties of train load frequencies and their applications, Journal of Sound and Vibration. 397 (2017) 123-140.

[5] X. Sheng, C.J.C. Jones, D.J. Thompson, A theoretical study on the influence of the track on train-induced ground vibration, Journal of Sound and Vibration. 272 (2004) 909-936.

[6] G. Lombaert, G. Degrande, J. Kogut, S. François, The experimental validation of a numerical model for the prediction of railway induced vibrations, Journal of Sound and Vibration. 297 (2006) 512–535.

[7] S.L. Grassie, R.W. Gregory, D. Harrison, K.L. Johnson, The dynamic response of railway track to high frequency vertical excitation, Journal of Mechanical Engineering Science. 24 (1982) 77-90.

[8] N. Vincent, D.J. Thompson, 1995, Track dynamic behaviour at high frequencies. Part 2: experimental results and comparisons with theory. Vehicle System Dynamics Supplement, 24, 100-114.

[9] A.P. de Man, Pin-pin resonance as a reference in determining ballasted railway track vibration behaviour, HERON 45(1), 35-51, 2000

[10] C.E. Inglis, The vertical path of a wheel moving along a railway track. Journal of the Institution of Civil Engineers, Paper 5201, pp262-277, March 1939.

[11] Belotserkovskiy PM. On the oscillations of infinite periodic beams subjected to a moving concentrated force. J Sound Vib 1996; 193: 705–712.

[12] A. Nordborg, Vertical rail vibration: parametric excitation, Acustica. 84 (1998) 289-300.

[13] A. Nordborg, Vertical rail vibration: point force excitation, Acustica. 84 (1998) 280-288.

[14] X. Sheng, C.J.C. Jones, D.J. Thompson, Responses of infinite periodic structures to moving or stationary harmonic loads, Journal of Sound and Vibration. 282 (2005) 125-149.

[15] T.X. Wu, D.J. Thompson, On the parametric excitation of the wheel/track system, Journal of Sound and Vibration. 278 (2004) 725-747.

[16] T. Mazilu, Green's functions for analysis of dynamic response of wheel/rail to vertical excitation. Journal of Sound and Vibration 306 (2007) 31–58.

[17] T. Mazilu, On the dynamic effects of wheel running on discretely supported rail. Proceedings of the Romanian Academy, Series A, Volume 10, Number 3 (2009)

[18] W. Zhai, Z. Cai, Dynamic interaction between a lumped mass vehicle and a discretely supported continuous rail track, Computers and Structures. 63 (1997) 987–997.

[19] N. Triepaischajonsak, D.J. Thompson, A hybrid modelling approach for predicting ground vibration from trains, Journal of Sound and Vibration. 335 (2015) 147-173.

[20] S.G. Koroma, D.J. Thompson, M.F.M. Hussein, E. Ntotsios, A mixed space-time and wavenumber-frequency domain procedure for modelling ground vibration from surface railway tracks, Journal of Sound and Vibration. 400 (2017) 508-532.

[21] M. Germonpré, J.C.O. Nielsen, G. Degrande, G. Lombaert, Contributions of longitudinal track unevenness and track stiffness variation to railway induced vibration, Journal of Sound and Vibration. 437 (2018) 292–307.

[22] J. Dai, K.K. Ang, M.T. Tran, V.H. Luong, D. Jiang, Moving element analysis of discretely supported high-speed rail systems. Proc IMechE Part F: J Rail and Rapid Transit 2018, Vol. 232(3) 783–797.

[23] H. Huang, S. Shen, E. Tutumluer, Moving load on track with Asphalt trackbed, Vehicle System Dynamics, 48:6, 737-749 (2010).

[24] P. Lou, X-G Zhong, J-F Tang, and Q-Y Zeng, Finite-element analysis of discretely supported rail subjected to multiple moving concentrated forces. Proc. IMechE Vol. 220 Part F: J. Rail and Rapid Transit, 305-315, 2006.

[25] L. Andersen, S. Nielsen, Vibrations of a track caused by variation of the foundation stiffness. Probab. Eng. Mech. 18, 171–184 (2003)

[26] J. Nielsen, A. Igeland, Vertical dynamic interaction between train and track influence of wheel and track imperfections, Journal of Sound and Vibration. 187 (1995) 825–839.

[27] Y.Q. Sun, M. Dhanasekar, A dynamic model for the vertical interaction of the rail track and wagon system, International Journal of Solids and Structures. 39 (2002) 1337–1359.

[28] J.C.O. Nielsen, G. Lombaert, S. Francois, A hybrid model for prediction of ground-borne vibration due to discrete wheel/rail irregularities, Journal of Sound and Vibration. 345 (2015) 103-120.

[29] C. Andersson, T. Dahlberg, Wheel/rail impacts at a railway turnout crossing. Proc Instn Mech Engrs Vol 212 Part F, 123-134, 1998

[30] V.L. Markine, M.J.M.M. Steenbergen, I.Y. Shevtsov, Combatting RCF on switch points by tuning elastic track properties. Wear 271 (2011) 158–167.

[31] K. Koro, K. Abe, M. Ishida, T. Suzuki, Timoshenko beam finite element for vehicle–track vibration analysis and its application to jointed railway track. Proc. Instn Mech. Engrs Vol. 218 Part F: J. Rail and Rapid Transit (2004) 159-172.

[32] S.C. Yang, Enhancement of the finite-element method for the analysis of vertical train–track interactions. Proc. IMechE Vol. 223 Part F: J. Rail and Rapid Transit, 609-620, 2009.

[33] A. Lubaschagne, N.F.J. van Rensburg, A.J. van der Merwe, Comparison of linear beam theories. Mathematical and Computer Modelling 49 (2009) 20-30.

[34] A.T. Beck, C.R.A. da Silva Jr., Timoshenko versus Euler beam theory: Pitfalls of a deterministic approach. Structural Safety 33 (2011) 19-25.

[35] A. Yavari, M. Nouri, M. Mofid, Discrete element analysis of dynamic response of Timoshenko beams under moving mass. Advanced Engineering Software 33 (2002) 143-153.

[36] A. Mosavi, R. Benkreif, A.R. Varkonyi-Koczy, Comparison of Euler-Bernoulli and Timoshenko Beam Equations for Railway System Dynamics. In D. Luca et al. (eds.), Recent Advances in Technology Research and Education, Advances in Intelligent Systems and Computing 660, 32-40, 2018.

[37] P. Ruge, C. Birk, A comparison of infinite Timoshenko and Euler–Bernoulli beam models on Winkler foundation in the frequency- and time-domain. Journal of Sound and Vibration 304 (2007) 932–947.

[38] K. Abe, Y. Chida, P.E.B. Quinay, K. Koro, Dynamic instability of a wheel moving on a discretely supported infinite rail. Journal of Sound and Vibration 333 (2014) 3413–3427

[39] X. Zhang, D.J. Thompson, Q. Li, D. Kostovasilis, M.G.R. Toward, G. Squicciarini, J. Ryue, A model of a discretely supported railway track based on a 2.5D finite element approach, Journal of Sound and Vibration. 438 (2019) 153-174.

[40] M.A. Heckl, Railway noise - can random sleeper spacings help? Acustica 81, 559-564, 1995.

[41] J. Ryue, D.J. Thompson, P.R. White, D.R. Thompson, Investigations of propagating wave types in railway tracks at high frequencies, Journal of Sound and Vibration. 315 (2008) 157-175.

[42] R. Ferrara, G. Leonardi, F. Jourdan, A contact-area model for rail-pads connections in 2-D simulations: sensitivity analysis of train-induced vibrations, Vehicle System Dynamics. 51(9) (2013) 1342-1362.

[43] T. Mazilu, M. Leu, Impact of the rail-pad multi-discrete model upon the prediction of the rail response, IOP Conference Series: Materials Science and Engineering. 227 (2017) 012079.

[44] B. Blanco, A. Alonso, L. Kari, N. Gil-Negrete, J. G. Giménez, Distributed support modelling for vertical track dynamic analysis, Vehicle System Dynamics. 56(4) (2018) 529-552.

[45] X. Sheng, M. Li, C.J.C. Jones, D.J. Thompson, Using the Fourier series approach to study interactions between moving wheels and a periodically supported rail, Journal of Sound and Vibration. 303 (2007) 873-984.